Measuring the Length of the Pore of the Sheep Cardiac Sarcoplasmic Reticulum Calcium-Release Channel Using Related Trimethylammonium Ions as Molecular Calipers

Andrew Tinker and Alan J. Williams

Department of Cardiac Medicine, National Heart and Lung Institute, University of London, London SW3 6LY, United Kingdom

ABSTRACT   After incorporation of purified sheep cardiac Ca^{2+}-release channels into planar phospholipid bilayers, we have investigated the blocking effects of a series of monovalent (CH_3-$(CH_2)_{n-1}$-$N^+(CH_3)_3$) and divalent (($CH_3)_3N^+$-$(CH_2)_n$-$N^+(CH_3)_3$) trimethylammonium derivatives under voltage clamp conditions. All the compounds tested produce voltage-dependent block from the cytoplasmic face of the channel. With divalent (Qn) derivatives the effective valence of block decreases with increasing chain length, reaching a plateau with a chain length of $n \geq 7$. No decline in effective valence is observed with the monovalent (Un) derivatives. A plausible interpretation of this phenomena suggests that for the 90% of the voltage drop measured, the increase in length following the addition of a CH_2 in the chain spans 12.7% of the electrical field. Extrapolating this distance to include the remaining 10% suggests that the applied holding potential falls over a total distance of 10.4 Å. In addition, at high positive holding potentials there is evidence for permeation of the trimethylammonium ions and a valency specific relief of block.

INTRODUCTION

The contractile state of cardiac and skeletal muscle cells is determined by the level of Ca^{2+} in the cytosol. On excitation, Ca^{2+} is released from its intracellular storage site, the sarcoplasmic reticulum (SR), through ion channels located in specialized regions of this membrane network (Bers, 1991). The Ca^{2+}-release channel has been isolated (Inui et al., 1987; Lai et al., 1988; Lindsay and Williams, 1991) and identified as an oligomeric protein with four identical monomers, each having a molecular weight of ~500 kD (Lai et al., 1988). Such is the size of the oligomer that it is possible to use ultrastructural techniques, including image reconstruction, to visualize the channel protein (Wagenknecht et al., 1989; Radermacher et al., 1992). Under these conditions, the SR Ca^{2+}-release channel displays fourfold symmetry and measures 27 × 27 × 14 nm. The structure appears to have a number of peripheral conducting vestibules at the cytoplasmic face which converge to a common channel at the luminal face.

Concurrent with the ultrastructural examination of the protein have been electrophysiological investigations. Current flow through single SR Ca^{2+}-release channels has been monitored following the reconstitution, into planar phospholipid bilayers, of either native junctional SR membrane vesicles or purified channel proteins (Smith et al., 1985; Lai et al., 1988; Ashley and Williams, 1990; Lindsay and Williams, 1991). Much of the literature describes regulation of channel gating by physiological and pharmacological agents (Williams, 1992; Meissner, 1994); however, Ca^{2+}

flux from the SR will also be influenced by the selectivity properties of the open pore. Therefore, we have made a detailed study of the permeation properties of the sheep cardiac Ca^{2+}-release channel (Tinker et al., 1992c; Tinker and Williams, 1993b). The picture that emerges from these investigations is of a channel that displays exceptionally high single-channel conductance with both divalent and monovalent cations as permeant species, but maintains a moderate degree of discrimination between the divalent and monovalent cations as groups (e.g., $pCa^{2+}/pK^+ = 6.5$).

How might these characteristics of ion handling be achieved? It is likely that a major determining factor will be the size of the region of the channel protein over which electrodiffusion can occur; in other words, how is physical distance related to the drop of potential across the conduction pathway and is this distance compatible with the structural information provided by the ultrastructural studies described above?

Miller (1982a) devised an elegant method for the measurement of the physical distance of the voltage drop using bis-quaternary ammonium blocking cations of varying length. The principle underlying this approach is to use the blocking cations as molecular calipers. One charged group marks the blocking position in the conduction pathway while the other is positioned at varying locations in the voltage drop, dependent on blocker length. The total effect is reflected in the effective valence of block. This approach has been used to monitor the length of the voltage drop in the SR K^+ channel and the Ca^{2+}-activated K^+ channel (Miller, 1982a; Villarroel et al., 1988).

There is an additional reason to study the interaction of organic cations of this structure with the conduction pathway of the cardiac SR Ca^{2+}-release channel. The mechanism that governs divalent-monovalent selectivity in this channel, for example Ca^{2+}-K^+, seems to be determined more by valency considerations than by ion-specific factors (Tinker et al., 1992a). Consequently, it should be of interest to determine

how monovalent and divalent blockers of similar structure behave. With these objectives in mind, we have investigated the blocking interactions of a series of related divalent and monovalent trimethylammonium cations.
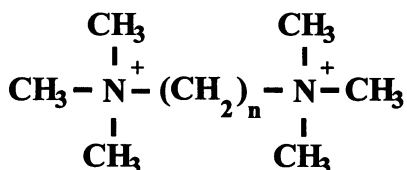
MATERIALS AND METHODS

Phosphatidylethanolamine was purchased from Avanti Polar Lipids (Alabaster, AL) and phosphatidylcholine from Sigma Ltd. (Poole, Dorset, UK). [^{3}H]ryanodine was obtained from New England Nuclear Ltd., (Boston, MA). Aqueous counting scintillant was purchased from Packard (Groningen, The Netherlands).

A series of related divalent and one monovalent trimethylammonium based blocking derivatives were examined. The convention used to describe them is summarized in Fig. 1. Q6 and Q10, better known as hexamethonium and decamethonium, were obtained as bromide salts from Aldrich Chemical Company (Standard Catalogue; Gillingham, Dorset, UK) and Q5 also from Aldrich Chemical Company (Rare and Fine Chemicals Catalogue). The other derivatives were synthesized as detailed below. All these ions were dissolved in the standard experimental 210 mM K$^+$ solution to make concentrated stock solutions from which small aliquots were added to the solutions in the *cis* and *trans* chambers. The other chemicals used were obtained as best available grade from BDH Ltd. (Dagenham, Essex, UK), Aldrich or Sigma.

Synthesis of the blocking derivatives

The derivatives Q3, Q4, Q7–Q9 were synthesized by reaction of the respective *n*-dibromoalkane with 5–6 molar excess of trimethylamine in acetonitrile. The mixture was refluxed for 6 h and the product either formed during the reflux period or dropped out of solution on cooling. U6 and U10 were synthesized by reacting the *n*-iodoalkane with 2–3 molar excess trimethylamine in ethanol. The mixture was refluxed for 48 h. The product did not spontaneously drop out of solution, but precipitated following the addition 2–3 volumes of ether. Q2 could not be synthesized by analogous methods, probably because of steric restraints. This derivative was made by reacting 5–6 molar excess methyliodide with *N,N,N',N'*-tetramethylethylenediamine using acetonitrile as a solvent. The mixture was refluxed for 24 h. All products were washed with ether and dried over

$$CH_3 - \overset{\overset{\displaystyle CH_3}{|}}{\underset{\underset{\displaystyle CH_3}{|}}{N}}{}^{+} - (CH_2)_n - \overset{\overset{\displaystyle CH_3}{|}}{\underset{\underset{\displaystyle CH_3}{|}}{N}}{}^{+} - CH_3$$

e.g. n=2 is Q2, n=10 is Q10 (decamethonium)

$$CH_3 - \overset{\overset{\displaystyle CH_3}{|}}{\underset{\underset{\displaystyle CH_3}{|}}{N}}{}^{+} - (CH_2)_{n-1} - CH_3$$
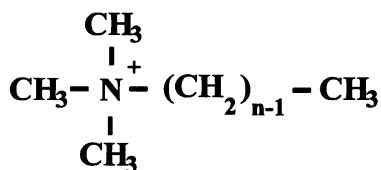
e.g. n=6 is U6

FIGURE 1   General structure of the blocking cations studied.

phosphorus pentoxide. The reagents for the above syntheses were obtained from Aldrich (Standard Catalogue) and Janssen Chimica (Beerse, Belgium). The chemical identity of the synthesized compounds was checked by NMR spectroscopy.

The distance between the two charged nitrogens in the Qn derivatives (N$^+$-N$^+$ distance) was measured using HyperChem (Release 3 for Windows; AutoDesk). The relevant Qn was minimized using the MM$^+$ force field and the N$^+$-N$^+$ distance measured using a mouse.

Preparation of sheep cardiac heavy sarcoplasmic reticulum (HSR) membrane vesicles

Sheep hearts were collected from a local abattoir or from Selborne Biological Services Ltd. in ice-cold cardioplegic solution (Tomlins et al., 1986). Homogenization of the ventricular septum and left ventricular free wall, followed by differential centrifugation, gives a mixed membrane fraction. This can be fractionated further on a discontinuous sucrose gradient yielding a HSR fraction at its 30/40% (w/v) interface (Sitsapesan and Williams, 1990). The HSR fraction was resuspended in 0.4 M KCl before sedimentation at 100,000 × g. The resulting pellet was resuspended in 0.4 M sucrose, 5 mM N'-2-hydroxyethylpiperazine-N'-2-ethanesulfonic acid (HEPES) titrated to pH 7.2 with hydroxymethyl methylamine (Tris).

Solubilization and separation of the ryanodine receptor

The solubilization of the ryanodine receptor by the zwitterionic detergent 3-[(3-cholamidopropyl)-dimethylammonio]-1-propane sulfonate, the subsequent separation of the receptor from other SR membrane proteins and the reconstitution of the receptor into unilamellar liposomes for incorporation into planar phospholipid bilayers were performed as described previously (Lindsay and Williams, 1991).

Planar lipid bilayer methods

Lipid bilayers, formed from suspensions of phosphatidylethanolamine in *n*-decane (35 mg/ml), were painted across a 200-μm diameter hole in a polystyrene copolymer partition which separated two chambers referred to as the *cis* (volume 0.5 ml) and *trans* (volume 1.5 ml) chambers. The *trans* chamber was held at virtual ground while the *cis* chamber could be clamped at various holding potentials relative to ground. Current flow across the bilayer was measured using an operational amplifier as a current-voltage converter as described by Miller (1982b). Bilayers were formed in solutions of 200 mM KCl, 20 mM HEPES, titrated with KOH to pH 7.4, resulting in a solution containing 210 mM K$^+$. An osmotic gradient was established by the addition of a small quantity (usually 50 to 100 μl) of 3 M KCl to the *cis* chamber. Proteo-liposomes were added to the *cis* chamber and stirred. To induce fusion of the proteo-liposomes with the bilayer a second small aliquot (50–100 μl) of 3 M KCl was added to the *cis* chamber. After channel incorporation, further fusion was prevented by perfusion of the *cis* chamber with 210 mM K$^+$. Solutions contained 10 μM free Ca^{2+} as contaminant, which was generally sufficient for channel activation. Very occasionally it was necessary to raise the Ca^{2+} in the *cis* chamber to 50–100 μM to obtain sufficient activation. Experiments were carried out at room temperature (21 ± 2°C).

The receptor-channel incorporates in a fixed orientation in the bilayer; the *cis* chamber corresponds to the cytosolic face of the channel and the *trans* to the luminal (Lindsay and Williams, 1991; Tinker et al., 1992a). In the subsequent discussion this naming convention will be adopted and current flowing from the cytoplasm to the interior of the SR referred to as positive to ground.

Single-channel data acquisition and analysis

Single-channel current fluctuations were displayed on an oscilloscope and stored on videotape. For analysis, data were replayed, filtered using an 8 pole

Bessel filter and digitized using an AT-based computer system (Satori, Intracel, Cambridge, UK). Single-channel current amplitudes and amplitude histograms were determined from digitized data. Single-channel current amplitudes were measured using manually controlled screen cursors to mark the open and closed levels. The data were filtered at 500–1000 Hz, depending upon the open channel noise in the presence of blocker and digitized at four times the filtering rate.

The blocking parameters given in Table 1 were calculated from nonlinear regression fits of the Woodhull equation (Woodhull, 1973) (Eq. 2) of mean relative conductance to holding potential using a commercially available program (Graphpad Inplot Ver. 4.03, GraphPad Software, San Diego, CA). The nonlinear regression program generates standard errors of the mean (SEM). However, these figures should be treated with caution as only approximate measures of data spread. Other approaches, such as linearization, may overestimate the importance of very small changes in relative conductance at negative holding potentials, a problem that may be particularly pronounced with very voltage-dependent blockers. In practice, these problems make only small differences to the blocking parameters finally obtained (Tinker and Williams, 1993a). Concentrations of blocking ions were chosen so that ~50% block was demonstrated at a holding potential of 40 mV.

The β function, as described by Fitzhugh (1983), Yellen (1984), and Quayle et al. (1988), was used to estimate the kinetics of Q10 and U6 block with the receptor channel. Briefly, the filter output of the open-to-blocked transition is a probability density function of the form

$$f(y) = \frac{y^{a-1} \cdot (1-y)^{b-1}}{\int_0^1 y^{a-1} \cdot (1-y)^{b-1} \cdot dy} \tag{1}$$

where a and b are related to the on (K_{on}) and off (K_{off}) rates and the filter time constant (τ) by $K_{on} = b/\tau$ and $K_{off} = a/\tau$. These equations only describe an output for a first-order filter. The frequency (f) of the Bessel filter is related to the effective time constant by $\tau = 0.228/f$. It relies on the compilation of an amplitude histogram predominantly from periods where the channel is open. Eq. 1 together with convolved and baseline noise is fitted to the amplitude histogram. For the analysis of Q10 block by this method, data were generally filtered at 1.5 kHz and for U6 at 2 kHz. Occasionally slightly harsher filtering was used so that a and b were >2. The practical details and validation of the approach were identical to those outlined previously (Tinker and Williams, 1993a).

RESULTS

As in our previous studies with the purified sheep cardiac SR Ca^{2+}-release channel (Tinker and Williams, 1993a), the experiments described here were performed with K^+ as the current carrier. In symmetrical 210 mM K^+, the current-voltage relationship is linear with a very large slope conductance of ~720 pS (Lindsay et al., 1991). Thus the signal-to-noise ratio is maximized.

Our laboratory has performed extensive characterizations of the conduction and blocking properties of the purified

sheep cardiac SR Ca^{2+}-release channel. The channel behaves to good approximation as though it can be occupied by at most one ion at a time (Tinker et al., 1992c). A number of tetra- and trimethylammonium derivatives (Tinker et al., 1992b; Tinker and Williams, 1993a) are able to produce voltage-dependent block, the kinetic behavior of which is consistent with interaction at a single site located 90% of the way across the voltage drop from cytosol to lumen of the SR. The objective of the current study was to extend our knowledge of the SR Ca^{2+}-release channel by estimating the physical length of the conduction pathway and by examining the influence of valency on blocker behavior.

The derivatives cause voltage-dependent block

In an analogous fashion to our previous studies, the addition of the derivatives to the cytoplasmic face of the channel results in a reduction of single-channel current which is most pronounced at positive holding potentials. The addition of comparable or higher concentrations of the trimethylammonium derivatives to the luminal face of the channel does not affect single-channel current amplitudes. However, to avoid problems with asymmetric surface potentials developing due to blocker binding to the bilayer on one side of the membrane (Miller, 1982a), the tested blocking cations were added to both chambers. The effects of the symmetrical addition of a series of selected blocking cations are illustrated in Fig. 2.

For the smaller derivatives (Q2-Q7) with single-channel records filtered at 1 kHz, the blocking effect was manifest as a reduction in current amplitude compared to control. The usual interpretation of such a phenomenon is that the entry and exit of the blocker are so much faster than the time resolution possible with the recording system that the channel-blocker interaction is time-averaged. The effects of the larger and/or more hydrophobic derivatives (Q8-Q10, U6) are similar, except that if records are filtered at 1 kHz or above, there is an excess of noise on the open channel current amplitude. This reflects the slower blocker kinetics of these larger/more hydrophobic derivatives. However, even with filtering corner frequencies of 4 kHz, it is impossible to convincingly demonstrate the direct entry and exit of the blocker in the conduction pathway. With Q8/Q9/U6 the data were filtered at 750/500/750 Hz, respectively, effectively leading to a smooth block to measure single-channel current amplitudes.

It is possible to combine the Boltzmann distribution and the Langmuir binding isotherm (Woodhull, 1973) to predict the change in relative conductance (g/g_o; the current in the presence of blocker divided by the control current) with variations in blocker concentration ([B]) and holding potential (V) given that the blocking site lies a fraction δ into the voltage drop. In the simplest treatment, the blocker, of valence z, is only able to gain access to the site from one side of the channel. The relative conductance is given by

$$\frac{g}{g_o} = 1 \left/ \left[1 + \frac{[B]}{K_b(0)} \exp\left(z\delta \frac{FV}{RT} \right) \right] \right. \tag{2}$$

TABLE 1 Calculated blocking parameters

Derivative	N^+-N^+ distance	n	Concentration (mM)	$z\delta \pm$ SEM	$K_b(0) \pm$ SEM (mM)
Q2	3.6 Å	4	2.5	1.60 ± 0.05	16.7 ± 1.3
Q3	5.2 Å	4	5	1.53 ± 0.06	43.5 ± 3.8
Q4	6.4 Å	4	7.5	1.29 ± 0.05	49.3 ± 4.0
Q5	7.7 Å	4	12.5	1.15 ± 0.04	47.6 ± 2.9
Q6	9.0 Å	4	5	1.09 ± 0.04	28.8 ± 1.9
Q7	10.3 Å	4	5	1.0 ± 0.04	34.3 ± 2.0
Q8	11.6 Å	4	3	1.06 ± 0.03	14.2 ± 1.4
Q9	12.8 Å	4	1	1.09 ± 0.04	6.93 ± 0.5
U6	/	4	5	0.89 ± 0.04	21.3 ± 1.4

+60 mV   -60 mV
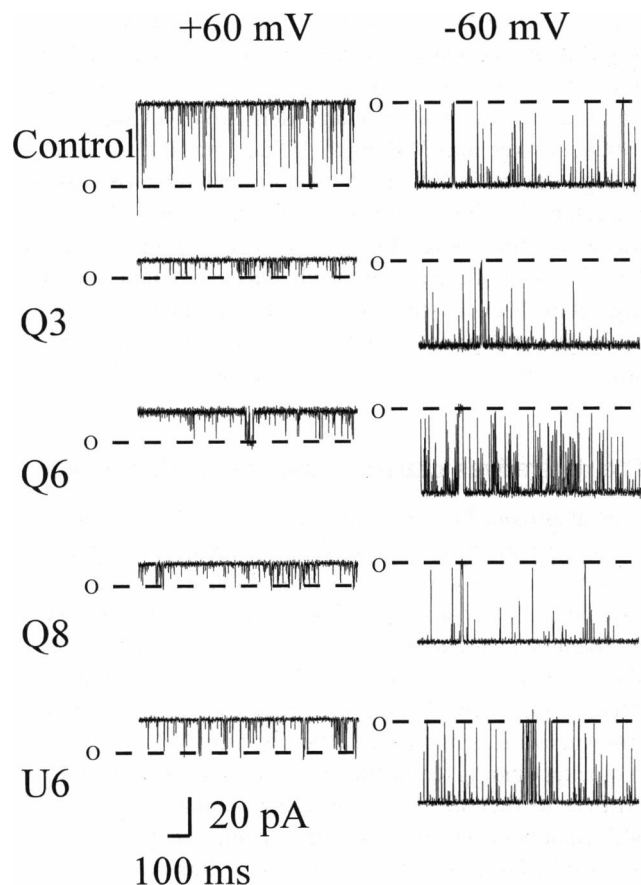

FIGURE 2   Representative single-channel current fluctuations at a holding potential of ±60 mV in the presence of symmetrical 5 mM Q3, 5 mM Q6, 3 mM Q8, and 5 mM U6. The control trace is from the Q6 experiment. The traces were filtered at 1 kHz (control, Q3, and Q6) or 750 Hz (Q8 and U6), digitized at 4 kHz, and generally chosen to show a single level. A brief opening of a second channel is apparent on the left control.

where $K_b(0)$ is the dissociation constant at 0 mV holding potential and $z\delta$ is conventionally referred to as the effective valence. F, R, and T have their usual meanings and RT/F is 25.2 mV at 20°C.

The change in relative conductance with holding potential was measured in 5-mV steps from ±15 to ±60 mV for the derivatives Q2-Q9 and U6. The above equation was fitted by nonlinear regression to the mean relative conductances. Fig. 3 shows the behavior of mean relative conductance with holding potential for Q2, Q4, and Q8, together with nonlinear regression fits to the Woodhull model. Table 1 gives the mean values of $z\delta$ and $K_b(0)$ obtained for the derivatives. The structural implications of these parameters are discussed later.

There is evidence for permeation of the blocking cation at high positive holding potentials

The simple Woodhull model provides an adequate description of the observed changes in relative conductance with holding potential up to 60 mV. Above this value the experimental points begin to deviate increasingly from the theoretical predictions. The tendency is much more pronounced
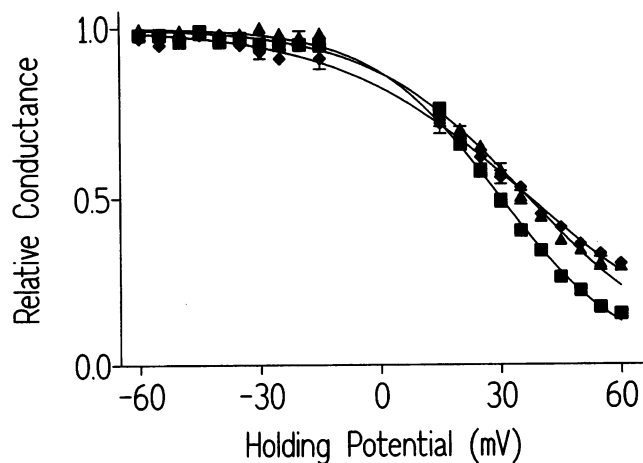

FIGURE 3   The variation of mean relative conductance with holding potential for the trimethylammonium derivatives Q2 (■), Q4 (▲), and Q8 (◆). The points are the mean of four observations (except Q4 at +55 mV and −55 mV, where $n = 3$ and Q8 at −50 mV and +15 mV, where $n = 3$) with SEM indicated by the error bars or included within the symbol. The curves are the best fit nonlinear regression curves of Eq. 2 to the data. The parameters are given in Table 1.

for divalent as opposed to monovalent blocking cations. Fig. 4 shows the behavior of mean relative conductance over an extended voltage range in the presence of Q6 and U6. The relationship for Q6 deviates markedly from the Woodhull model, with a rising phase above 60–70 mV. Other divalent members of the group show a similar effect. With U6, relative conductance continues to decline, but this decline is not as steep as would be predicted from the Woodhull model with a $z\delta$ of 0.9.

It is possible to investigate the kinetic basis of this effect in more detail by using amplitude distribution analysis to estimate the variation in the on and off rate constants (K_{on} and
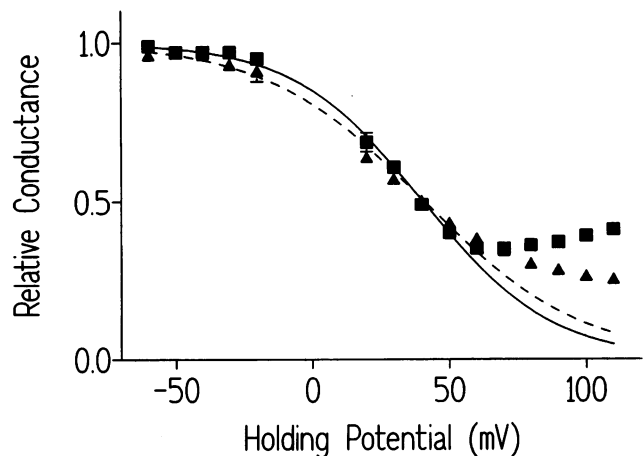

FIGURE 4   The variation of mean relative conductance with holding potential for the trimethylammonium derivatives Q6 (■; ——) and U6 (▲; - - - -). The curves are the best fit nonlinear regression curves of Eq. 2 to the data over the more limited range of ±60 mV. The parameters are given in Table 1. The points are the mean of four observations with SEM. indicated by the error bars or included within the symbol.

K_{off}) of the blocker with changing holding potential. By filtering the data at comparatively higher corner frequencies, it is possible to analyze excess noise on the open state to determine kinetic parameters (see Materials and Methods). Q6 leads to relatively smooth block, even with filtering at 2 kHz. As a result Q10 was chosen as the divalent cation to be analyzed. Interestingly, there is an excess of noise on the open state in the presence of U6 at positive holding potentials and this cation was used as the example monovalent cation for analysis. The broadening of the open channel noise in the presence of blocker with the fitted theoretical function is illustrated in Fig. 5. U10 was synthesized but the addition of this compound to the channel led to a pronounced decline in single-channel P_o, making it difficult to study. The effects of U10 may be analogous to experimental observations made in studies of the single-channel effects of procaine (Xu et al., 1993; Zahradníková and Palade, 1993).

The variation of K_{on} and K_{off} with holding potential was examined between 30 and 110 mV in 10-mV steps in the presence of either 200 μM Q10 or 5 mM U6. The mean results are presented in Fig. 6, A and B. One striking feature is the difference in the behavior of K_{off} with the two blocking cations. In the presence of U6, K_{off} is largely independent of holding potential. In contrast, for Q10, the relationship of K_{off} to holding potential has two components. At voltages below 60 mV, K_{off} is essentially independent of holding potential. Above this voltage, K_{off} increases with increasing voltage, behavior which is consistent with relief of block. This valency-specific difference in behavior will be discussed later.

If K_{on} is described by the Boltzmann relationship, then

$$K_{on}(V) = K_{on}(0) \cdot \exp\left(z_{on} \cdot \frac{FV}{RT}\right) \quad (3)$$

where $K(V)$ and $K(0)$ refer to the rate constant at a particular voltage and at 0 mV, respectively. z is the valence of the reaction. From a plot of the natural logarithm of the rate constant against holding potential it is possible to determine z from the slope and K(0) from the intercept. If linear regression is performed over the entire voltage range then the slopes are 0.0136 ± 0.0015 (± SEM; equivalent to a valency of 0.34) and 0.0218 ± 0.0015 (± SEM; equivalent to a valency of 0.55) and intercepts 5.13 ± 0.12 (± SEM; equivalent to an on rate at 0 mV of 169 ms^{-1}) and 1.94 ± 0.11 (± SEM; equivalent to an on rate at 0 mV of 6.95 ms^{-1}) for U6 and Q10, respectively. A more critical inspection of the data reveals that at higher potentials the slope seems to be leveling off (Fig. 6 C). This can be demonstrated by excluding the data points above 80 mV for U6 and 70 mV for Q10 and performing linear regression over a more limited range (*dashed lines*). The slopes obtained are then 0.0195 ± 0.0020 and 0.0282 ± 0.0037, respectively, for U6 and Q10. The implications of this finding will be discussed later.

The complex nature of the behavior of K_{off} with Q10 and to a much lesser extent U6, makes a similar determination of the valency of the kinetics less reliable given the small number of points measured before the plateau region at 60 mV.

DISCUSSION

Estimating the physical length of the voltage drop in the sheep cardiac SR Ca^{2+}-release channel

Fig. 7 A shows the behavior of $z\delta$ for the Qn series as chain length varies. Unlike the Un series, also shown in Fig. 7 A, $z\delta$ of the Qn series is not constant at 0.9; once the chain length shortens below 7 carbons, $z\delta$ increases. It is possible to use an explanation similar, in principle, to that first used by Miller (1982a) in his experiments with the Qn series in the rabbit skeletal SR K$^+$ channel. The Un series of blockers bind to a blocking site located 90% of the way across the voltage drop and thus have a $z\delta$ of 0.9. The members of the Qn series in which the second unbound trimethylammonium group is located outside the voltage drop, will behave, at least theoretically, in a similar fashion. As the chain length shortens the second charged group will come under the influence of the electric field and $z\delta$ rises. Using this approach it is possible to map the physical length of the voltage drop. If a linear regression line is fitted to the data for the Q7 to Q2 derivatives, then 12.7% of the voltage drop corresponds to the addition of a CH$_2$ group to the chain. By plotting the data given for the N$^+$-N$^+$ distance for Q2 to Q7 in Table 1 it is apparent that it changes on average 1.32 Å for the addition of each CH$_2$ group. On the assumption that the voltage drop is linear, this leads to an estimate that the electrical potential falls over a distance of only 10.4 Å in the cardiac Ca^{2+}-release channel. This estimate does not include any potentials from fixed negative charges that may extend further into the solution.

How do these measurements, obtained by electrophysiological methods, compare with the structure of the channel protein determined from image reconstruction? Our estimate of 10.4 Å for the length over which potential
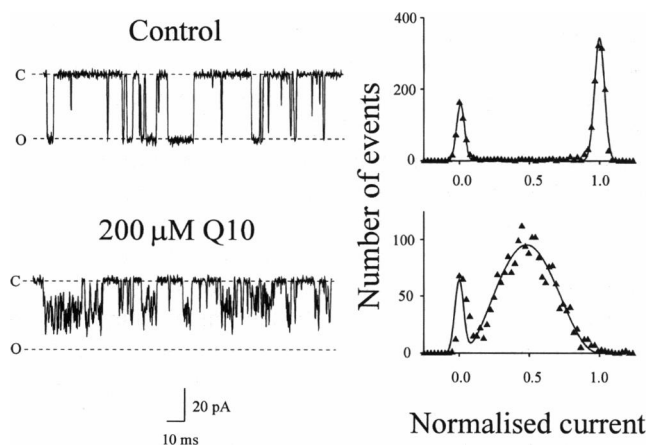

FIGURE 5   Diagram of the increase of open channel noise in the presence of Q10 at a holding potential of 60 mV (*left*). This is accompanied by a broadening of the amplitude histogram (right). Only openings where the channel was open for a significant period of time (at least 10 ms) were compiled into amplitude histograms. The data were filtered at 1.5 kHz and digitized at 6 KHz. Note the faster time base than in Fig. 2. The peaks in the amplitude histogram are fitted to the best-fit Gaussian distribution for control and the best fit β-function convolved with noise ($a = 3.36$ and $b = 3.56$; see Materials and Methods) in the presence of 200 μM Q10.
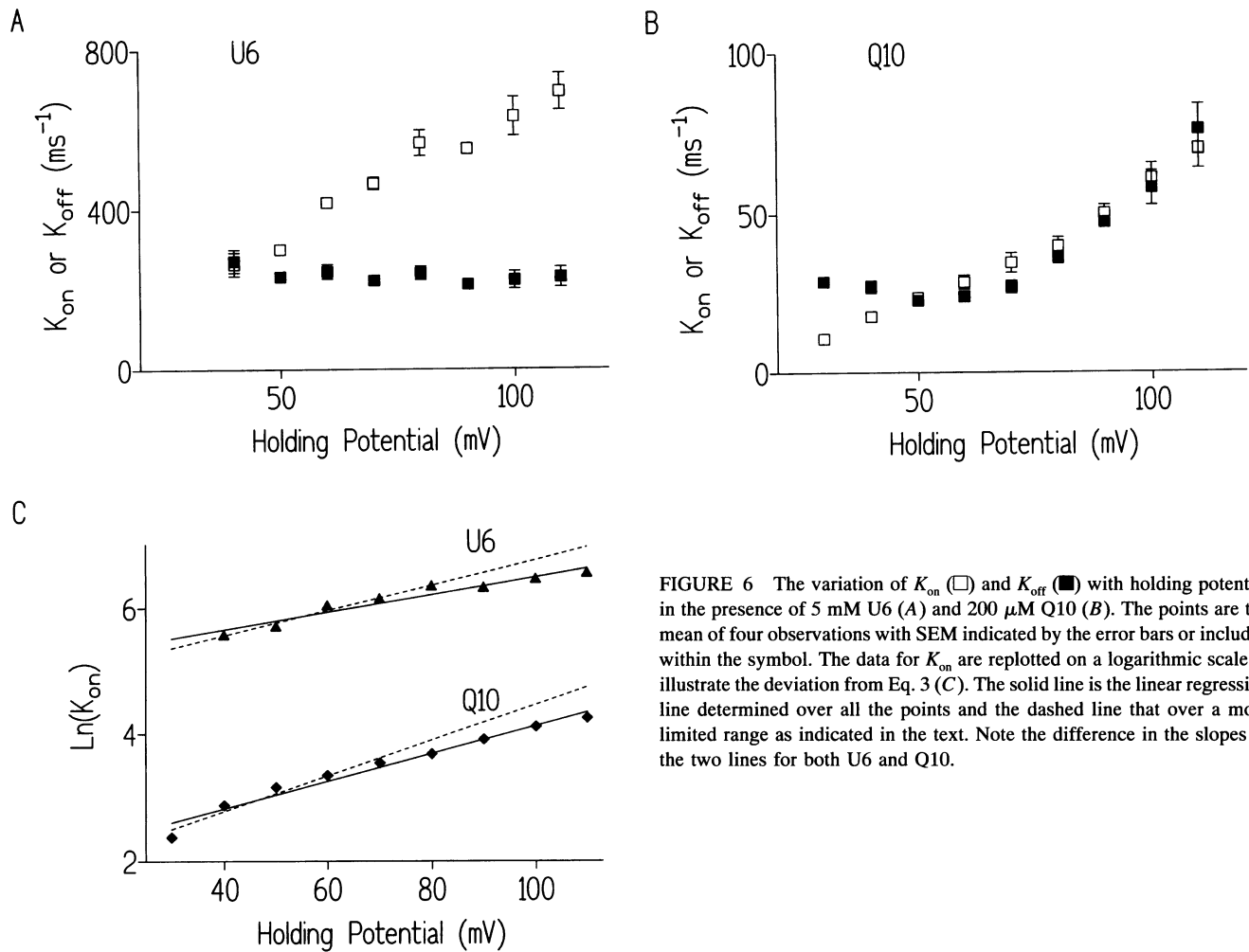
A

B

C

FIGURE 6   The variation of K_{on} (□) and K_{off} (■) with holding potential in the presence of 5 mM U6 (A) and 200 μM Q10 (B). The points are the mean of four observations with SEM indicated by the error bars or included within the symbol. The data for K_{on} are replotted on a logarithmic scale to illustrate the deviation from Eq. 3 (C). The solid line is the linear regression line determined over all the points and the dashed line that over a more limited range as indicated in the text. Note the difference in the slopes of the two lines for both U6 and Q10.

drops across the channel, together with the 3.5 Å radius obtained for the selectivity filter of the channel from our previous studies (Tinker and Williams, 1993b), suggests that ion discrimination is determined over a very short region, at most three or four turns of an α-helix. Even with the high levels of resolution available in current ultrastructural studies (3 nm), it would be impossible to visualize this region.

The method of analysis used here is valid if the channel can hold no more than one ion at a time. Our laboratory has performed a series of studies which largely support this hypothesis (Tinker et al., 1992c). Specifically blockers acting at the site located 90% of the way across the voltage drop behave as though binding to a single site: the Hill coefficients for the concentration dependence of block are close to 1 and the $z\delta$ of block is independent of concentration (Tinker and Williams, 1993a). It seems then that such an analysis is valid in the sheep cardiac Ca^{2+}-release channel. One small discrepancy arising from the current study is that, although the values of $z\delta$ of the Qn derivatives level off for Q7 to Q9, they do not quite reach the predicted value of 0.9 but are closer to 1.0–1.1 (Table 1). It seems probable that at the cytoplasmic face

of the Ca^{2+}-release channel there are wide vestibules over which a proportion of the voltage drop falls. The difference between the predicted and observed values of $z\delta$ may reflect some mobility of the unbound charged trimethylammonium group which enables it to move in and out of the voltage drop in such a wide vestibule.

A second interesting experimental observation is the behavior of the $K_b(0)$ with varying chain length shown in Fig. 7 B. $K_b(0)$ for the Qn derivatives rises with increasing chain length, reaching a peak at $n = 7$, and then declines. This is in contrast to the apparent steady decline of $K_b(0)$ with increasing chain length seen with the Un blocking cations (Tinker et al., 1992b). Indeed the dependence of $K_b(0)$ on chain length with the Un derivatives and tetraalkylammonium cations supports the importance of a largely hydrophobic interaction at this site. How could the position of the second unbound trimethylammonium group in the Qn derivatives influence the binding affinity? In addition to the site located at the luminal side of the channel, our earlier studies also support the existence of a second more centrally placed binding site which interacts with divalent cations and the blocking cation tetramethylammonium (Tinker et al., 1992a; Tinker et al., 1992c). If the second trimethylammonium
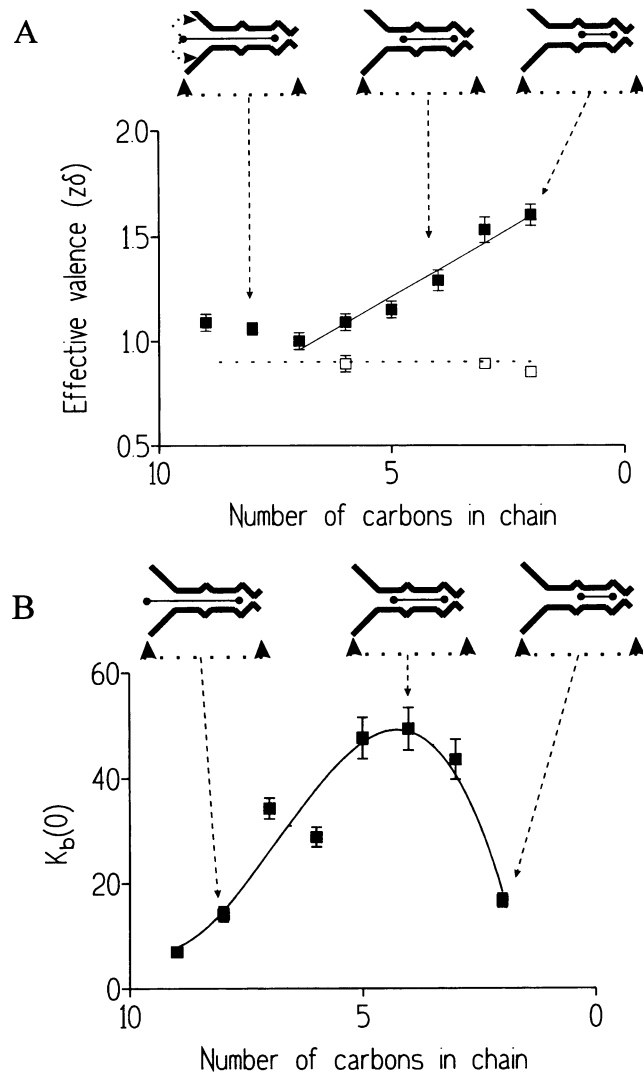
A

B

FIGURE 7   The variation of $z\delta$ (A) and $K_b(0)$ (B) with variations in blocker chain length. (■) Divalent derivative data points; (□) monovalent derivatives. The parameters for U2 and U3 were obtained from our previous study (Tinker et al., 1992a). The SEM is shown by the error bars or included within the symbol if smaller. The cartoons above the diagram indicate the possible positions of the divalent derivatives of varying chain length in the voltage drop (arrows below diagram). The large vestibule (left) is meant to represent the cytosolic face of the channel. The two binding sites are present to represent the divalent and hydrophobic binding sites identified from our previous studies (Tinker et al., 1992a; Tinker and Williams, 1993b).

group was significantly influenced by binding at this site in, for example, Q2 and Q3, then this may result in a lower $K_b(0)$ than would be expected from the trend over the falling phase with the larger derivatives (see Fig. 7 B).

Biophysical comparisons with other ion channels

Studies of the kind reported here have previously been carried out on the SR K^+ channel from rabbit skeletal muscle and the large conductance Ca^{2+}-activated K^+ channel from rat skeletal muscle (Miller, 1982a; Villarroel et al., 1988). The estimated length of the voltage drop in these channels,

calculated on the basis of linear variation of membrane potential with distance, was 10 Å and 35–40 Å, respectively. An advantage of our study is that we are measuring 90% of the voltage drop of the SR Ca^{2+}-release channel. In the studies of the SR K^+ channel, the blocking site was located 66% into the electrical field and in the Ca^{2+}-activated K^+ channel, 27%. A comparison of these results would suggest that the voltage drop is physically shorter in the sheep cardiac Ca^{2+}-release channel and the SR K^+ channel than in the Ca^{2+}-activated K^+ channel. A longer pore may be necessary for the Ca^{2+}-activated K^+ channel to bind multiple K^+ ions; in other words, for it to function as a multi-ion pore. There is good evidence that both the skeletal SR K^+ and cardiac SR Ca^{2+}-release channels function as single-ion channels. It may be that electrostatic repulsion in the shorter pore of these two channels will prevent it from becoming occupied by more than one ion at a time. Another consequence is that a short pore, by reducing channel resistance, will tend to maximize single-channel conductance. This parameter is strikingly large in the SR Ca^{2+} channel and makes it well suited for its role as a pathway for the release of Ca^{2+}. Structurally, the short physical distance of the voltage drop may be achieved by an hourglass-shaped pore which widens abruptly at either side of a constriction, so that channel resistance quickly approaches that of the bulk solution.

Other differences exist between our findings and those of similar previous studies on other channels. In the rabbit skeletal SR K^+ channel, Miller (1982a) observed a sharp increase in $z\delta$ with chain lengths in excess of 8, and this was interpreted as suggesting the additional binding of the second trimethylammonium group to the blocking site located 66% into the electric field. We observed no such increase in $z\delta$ in the SR Ca^{2+}-release channel, and this may reflect a lack of accessibility of the binding site, located 90% of the way across the voltage drop, to the second charged group. The variation of the $K_b(0)$ with increasing chain length in the studies of the SR K^+ channel and the sarcolemmal Ca^{2+}-activated K^+ channel was also compatible with a purely hydrophobic interaction, unlike the more complex relationship described in this study.

The blocking behavior at high positive potentials

To further complicate the picture, at holding potentials above 60 mV, we observed deviation from a Woodhull model in which the blocker is effective from only one side of the channel. In the Appendix we present an argument based on modeling that suggests that there is a second voltage-dependent transition that results in the bound "blocking" cation exiting into the lumen of the SR. The difference in behavior between monovalent and divalent cations is explained by two general factors. Most importantly, a long chain divalent Qn cation, unlike a similar length Un cation, must have the second unbound charged trimethylammonium group moved through a significant proportion of the voltage drop before exiting into the bulk solution corresponding to the lumen of the SR (see Fig. 8 A in Appendix). This would result in the exiting re-
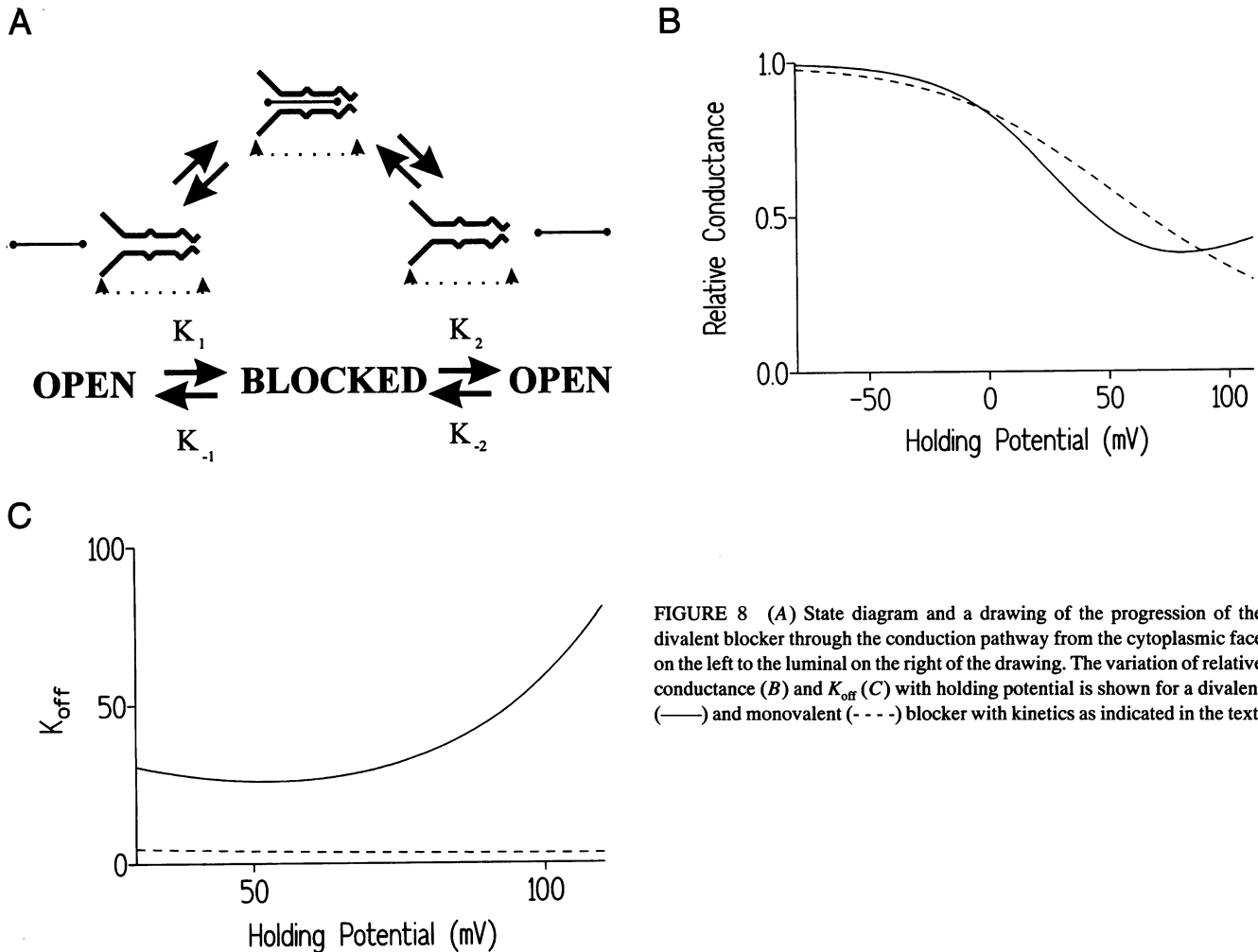
A

B

C

FIGURE 8 (A) State diagram and a drawing of the progression of the divalent blocker through the conduction pathway from the cytoplasmic face on the left to the luminal on the right of the drawing. The variation of relative conductance (B) and K_{off} (C) with holding potential is shown for a divalent (——) and monovalent (- - - -) blocker with kinetics as indicated in the text.

action having a much larger $z\delta$ for a divalent as opposed to a monovalent cation and would, in turn, lead to a much more significant relief of block with holding potential with divalents. In addition, to account for the effect with a monovalent such as U6, it is necessary to assume that if the exiting reaction in the absence of electrical driving force is of the same order of magnitude for mono- and divalent blocking cations, then the initial binding and unbinding rates must be slower than for a comparable divalent blocker. The absence of significant noise on the open channel level for Q6 as opposed to U6 and our previous studies showing that current-carrying alkaline earths appear to encounter less of an energetic barrier in traversing the channel than the group Ia cations (Tinker et al., 1992a) support this contention. The failure to observe any blocking effect following luminal addition of the blocking cations, even at negative holding potentials, may arise from two factors. The relatively higher energy barrier encountered at the luminal face of the channel and the location of the blocking site in the electric field would mean that the $K_b(0)$ will be higher and the $z\delta$ of block smaller, from the luminal side of the channel.

In addition to translocation of the blocking cations, other factors may contribute to the deviation of the relationship

between relative conductance and voltage from the Woodhull model. It is apparent from Fig. 6 C that the relationship between holding potential and K_{on} begins to level off at high positive holding potentials. This behavior is compatible with diffusion limitation (Läuger, 1976; Andersen, 1983). In other words, the rate of arrival of the blocking cation at the channel capture radius is determined by diffusion, and this begins to limit the subsequent transport by electrodiffusion of the blocker to its site of action in the channel. A more rigorous test of this possibility would involve maneuvers designed to change the diffusion properties of the solution.

In conclusion, we have used a series of monovalent and divalent trimethylammonium cations as molecular calipers to monitor the physical distance over which ion selectivity is determined in the cardiac SR Ca^{2+}-release channel. The estimated distance, 10.4 Å, is compatible with single-ion occupancy and high single-channel conductance for the channel. Taken together with our earlier estimate of the radius of the selectivity filter of 3.5 Å, this result suggests that the region of the channel responsible for ion discrimination is not equivalent to the structural features seen in recent ultrastructural investigations. In addition to structural data, these stud-

ies have demonstrated permeation of blocking cations at high holding potentials and have provided further information on the differences in the behavior of divalent and monovalent species in the channel.

APPENDIX

Consider the situation in Fig. 8 A. A blocker binding at the site located 90% of the way into the voltage drop can have two fates; it can either re-trace its steps and leave the channel to the cytoplasmic solution or it can permeate the channel and enter the solution equivalent to the lumen of SR. This can be represented by the state diagram in Fig. 8 A. Each of these steps has rates and each, at least theoretically, can have some voltage dependence. At a given holding potential (V) the fraction of channels blocked will be

$$\frac{(K_{-1}(V) + K_2(V))}{(K_{-1}(V) + K_1(V) + K_{-2}(V) + K_2(V))}. \tag{4}$$

In addition, the dwell time rate constant in the blocked state will be determined by the sum of the rates of the exiting pathways (Colquhoun and Hawkes, 1983) and will be given by

$$K_{off}(V) = K_{-1}(0) \cdot \exp\left(-z_{-1} \cdot \frac{FV}{RT}\right) + K_2(0) \cdot \exp\left(z_2 \cdot \frac{FV}{RT}\right) \tag{5}$$

where z_1, z_{-1}, z_2, and z_{-2} are the valencies of the respective reactions.

To use such a model to illustrate the findings of this study, some assumptions are necessary. Two blockers similar to U6 and Q6 are considered. Rates are considered, i.e., a fixed concentration of blocker is assumed and the units are not specified. However, rates for the divalent blocking cation are broadly similar to those seen for Q10. The intention was to reproduce the major qualitative trends. The rate constants depend on holding potential as described in Eq. 3. For the monovalent blocker, K_1 and K_{-1} must have a total voltage dependence of 0.9 and for a divalent blocker such as Q6, total voltage dependence must be 1.1. Arbitrarily, K_1 and K_{-1} were assumed to be equally voltage-dependent. This is probably not entirely accurate. Our studies with the monovalent local anesthetics suggested that K_{on} was responsible for much of the voltage dependence (Tinker and Williams, 1993a). However, divalent blockers are likely to behave differently, and for monovalent blockers the conclusions are not altered if K_{-1} is assumed to be independent of voltage (if anything the theoretical curves follow the observed data more closely). In addition, the voltage-dependence of the K_2/K_{-2} equilibrium is assumed to lie totally in K_2 on account of the failure to see any blocking effect at negative holding potentials with the blocker at the luminal face of the channel. The parameters used in the modeling are given in Table 2.

The basic difference between the two blocking cations lies in the voltage dependence of K_2 and the magnitude of K_1 and K_{-1}. The former especially accounts for the difference seen theoretically between the monovalent and

divalent cations and physically corresponds largely to the necessity of moving the second unbound charged trimethylammonium group 80% of the way across the voltage drop to clear the channel of blocker (Fig. 8 A).

The theoretical predictions for the behavior of the monovalent and divalent blocker are shown in Fig. 8, B and C. The simple scheme is able to reproduce the complex variation of relative conductance with holding potential seen with the divalent but not seen with the monovalent blocker (Fig. 8 B) and the similar behavior found in K_{off} (Fig. 8 C).

REFERENCES

Andersen, O. S. 1983. Ion movement through gramicidin A channels. Studies on the diffusion-controlled association step. *Biophys. J.* 41: 147–165.

Ashley, R. H., and A. J. Williams. 1990. Divalent cation activation and inhibition of single calcium release channels from sheep cardiac sarcoplasmic reticulum. *J. Gen. Physiol.* 95:981–1005.

Bers, D. M. 1991. Excitation-Contraction Coupling and Cardiac Contractile Force. Kluwer, Dordrecht. the Netherlands.

Colquhoun, D., and A. G. Hawkes. 1983. The principles of the stochastic interpretation of ion-channel mechanisms. *In* Single-Channel Recording. B. Sakmann and E. Neher, editors. Plenum Press, New York. 135–175.

Fitzhugh, R. 1983. Statistical properties of the asymmetric random telegraph signal, with application to single-channel analysis. *Math. Biosci.* 64: 75–89.

Inui, M., A. Saito, and S. Fleischer. 1987. Isolation of the ryanodine receptor from cardiac sarcoplasmic reticulum and identity with the feet structures. *J. Biol. Chem.* 262:15637–15642.

Lai, F. A., H. P. Erickson, E. Rousseau, Q-Y. Liu, and G. Meissner. 1988. Purification and reconstitution of the Ca release channel from skeletal muscle. *Nature.* 331:315–319.

Läuger, P. 1976. Diffusion-limited ion flow through pores. *Biochim. Biophys. Acta.* 455:493–509.

Lindsay, A. R. G., S. D. Manning, and A. J. Williams. 1991. Monovalent cation conductance in the ryanodine receptor-channel of sheep cardiac muscle sarcoplasmic reticulum. *J. Physiol.* 439:463–480.

Lindsay, A. R. G., and A. J. Williams. 1991. Functional characterization of the ryanodine receptor purified from sheep cardiac muscle sarcoplasmic reticulum. *Biochim. Biophys. Acta.* 1064:89–102.

Meissner, G. 1994. Ryanodine receptor/Ca^{2+} release channels and their regulation by endogenous effectors. *Annu. Rev. Physiol.* 56:485–508.

Miller, C. 1982a. Bis-quaternary ammonium blockers as structural probes of the sarcoplasmic reticulum K^+ channel. *J. Gen. Physiol.* 79:869–891.

Miller, C. 1982b. Open-state substructure of single chloride channels from *Torpedo electroplax. Phil. Trans. R. Soc. Lond. B.* 299:401–411.

Quayle, J. M., N. B. Standen, and P. R. Stanfield. 1988. The voltage-dependent block of ATP-sensitive potassium channels of frog skeletal muscle by caesium and barium ions. *J. Physiol.* 405:677–698.

Radermacher, M., T. Wagenknecht, R. Grassucci, J. Frank, M. Inui, C. C. Chadwick, and S. Fleischer. 1992. Cryo-EM of the native structure of the calcium release channel/ryanodine receptor from sarcoplasmic reticulum. *Biophys. J.* 61:936–940.

Sitsapesan, R., and A. J. Williams. 1990. Mechanisms of caffeine activation of single calcium-release channels of sheep cardiac sarcoplasmic reticulum. *J. Physiol.* 423:425–439.

Smith, J. S., R. Coronado, and G. Meissner. 1985. Sarcoplasmic reticulum contains adenine nucleotide-activated calcium channels. *Nature.* 316:446–449.

Tinker, A., A. R. G. Lindsay, and A. J. Williams. 1992a. Block of the sheep cardiac sarcoplasmic reticulum Ca^{2+}-release channel by tetraalkyl ammonium cations. *J. Membrane Biol.* 127:149–159.

Tinker, A., A. R. G. Lindsay, and A. J. Williams. 1992b. Large tetraalkyl ammonium cations produce a reduced conductance state in the sheep cardiac sarcoplasmic reticulum Ca^{2+}-release channel. *Biophys. J.* 61:1122–1132.

Tinker, A., A. R. G. Lindsay, and A. J. Williams. 1992c. A model for ionic conduction in the ryanodine receptor-channel of sheep cardiac muscle sarcoplasmic reticulum. *J. Gen. Physiol.* 100: 495–517.

TABLE 2 Parameters used in model

	K_1	K_{-1}	K_2	K_{-2}
Monovalent $K(0)$	1.0	5.0	1.5	0.25
Monovalent valency	0.45	0.45	0.1	0.0
Divalent $K(0)$	10.0	50.0	1.5	0.25
Divalent valency	0.55	0.55	0.9	0.0

Tinker, A., and A. J. Williams. 1993a. Charged local anesthetics block ionic conduction in the sheep cardiac sarcoplasmic reticulum calcium-release channel. *Biophys. J.* 65:852–864.

Tinker, A., and A. J. Williams. 1993b. Probing the structure of the conduction pathway of the sheep cardiac sarcoplasmic reticulum calcium-release channel with permeant and impermeant organic cations. *J. Gen. Physiol.* 102:1107–1129.

Tomlins, B., S. E. Harding, M. S. Kirby, P. A. Poole-Wilson, and A. J. Williams. 1986. Contamination of a cardiac sarcolemmal preparation with endothelial plasma membrane. *Biochim. Biophys. Acta.* 856: 137–143.

Villarroel, A., O. Alvarez, A. Oberhauser, and R. Latorre. 1988. Probing a Ca^{2+}-activated K^+ channel with quaternary ammonium ions. *Pflugers Arch. Eur. J. Physiol.* 413:118–126.

Wagenknecht, T., R. Grassucci, J. Frank, A. Saito, M. Inui, and S. Fleischer.

1989. Three-dimensional architecture of the calcium channel/foot structure of sarcoplasmic reticulum. *Nature.* 338:167–170.

Williams, A. J. 1992. Ion conduction and discrimination in the sarcoplasmic reticulum ryanodine receptor/calcium-release channel. *J. Muscle Res. Cell Motil.* 13:7–26.

Woodhull, A. M. 1973. Ionic blockage of sodium channels in nerve. *J. Gen. Physiol.* 61:687–708.

Xu, l., R. Jones, and G. Meissner. 1993. Effects of local anesthetics on single channel behavior of skeletal muscle calcium release channel. *J. Gen. Physiol.* 101:207–233.

Yellen, G. 1984. Ionic permeation and blockade in Ca^{2+}-activated K^+ channels of bovine chromaffin cells. *J. Gen. Physiol.* 84:157–186.

Zahradníková, A., and P. Palade. 1993. Procaine effects on single sarcoplasmic reticulum Ca^{2+} release channels. *Biophys. J.* 64:991–1003.